Inhibiting CBX4 efficiently suppress YAP nucleus translocation in hepatocellular carcinoma cells to protect against sorafenib resistance

wei zhao (linelong@126.com)

Key Laboratory of Carcinogenesis and Translational Research (Ministry of Education), Peking University Cancer Hospital & Institute https://orcid.org/0000-0001-6732-9466

BO Ma

beijing cancer hospital

Zhihua Tian

Beijing Cancer Hospital

Haibo Han

Beijing Cancer Hospital

Jintian Tang

Xinjiang Medical University Affiliated Tumor Hospital

Bin Dong

Beijing Cancer Hospital

Guo An

Beijing Cancer Hospital

Baoshan Cao

Peking University Third Hospital

Boqing Wang

Xinjiang Medical University Affiliated Tumor Hospital

Research

Keywords: hepatocellular carcinoma, sorafenib resistance, CBX4, YAP, miR424

Posted Date: May 5th, 2020

DOI: https://doi.org/10.21203/rs.3.rs-25977/v1

Abstract

Background

The discovery of biomarkers that predict the response to sorafenib and increase the efficiency of drug therapy represents a clinical challenge. This study aimed to investigate the possible role of inhibiting CBX4 to deregulate of CSCs and to evaluate the contribution of these molecules to sorafenib resistance in advanced HCC.

Methods

HCC cell lines and a xenograft mouse model with resistance to sorafenib were employed to analyze the effects of miR424 on CSC characteristics. RNA expression was analyzed by RT-PCR and next-generation sequencing in a cohort of 106 HCC cancer patients and sorafenib-resistant (SR) cell lines, respectively, to validate the key microRNAs and targets in the network. CBX4 expression was determined in HCC cells to examine YAP1-mediated stem-cell-like activation and its association with sorafenib resistance.

Results

MicroRNA and mRNA profiles of SR cell lines identified miR424 and its direct target CBX4 as significantly associated with stem-cell-like properties, poor survival and clinical characteristics. Functional experiments demonstrated that miR424 suppressed CBX4, and CBX4 induced nuclear translocation of YAP protein but was not associated with protein production. When YAP1 and CBX4 were modulated either alone or together in SR tumors with CA3 and UNC3866, respectively, tumorigenicity and stem-like properties were extremely inhibited, thus indicated that these compounds exerted a strong antitumor effect in vivo against SR HCC cells.

Conclusions

Our results revealed that blocking the crosstalk between CBX4 and YAP1 is critical in response to sorafenib resistance, and it could be a promising therapeutic strategy for patients with advanced HCC.

1. Introduction

Hepatocellular carcinoma (HCC) is the fourth leading cause of cancer death worldwide (8.2% of all cancer-related deaths), with increasing incidence and high mortality[1]. HCC is difficult to diagnose in its early stage and has poor survival because of its high frequency of recurrence, metastasis after hepatectomy, and resistance to common chemotherapy[2]. Sorafenib, an oral multikinase inhibitor, is currently regarded as a first-line systemic treatment option in patients with advanced HCC due to its potential to provide a survival advantage of 2–3 months based on the results of two phase III clinical

trials[3, 4]. Although the treatment has significant increased mean overall survival (OS), the high resistance rate has significantly limited the benefit of sorafenib therapy. Previous studies have reported that enrichment of cancer stem cells (CSCs) may contribute to sorafenib resistance after initial treatment years prior[5, 6]. However, the molecular mechanism by which CSCs affect sorafenib efficacy in HCC are still unclear, and it remains to be elucidated if CSCs play a role in the regulation of drug resistance in HCC. Therefore, exploring the development and evolution of targeted drug resistance is very important to improve the efficacy of HCC chemotherapy.

Chromobox homolog 4 (CBX4), also known as polycomb 2 (PC2) or NBP16, is located on chromosome 17q25.3 and encodes a polycomb repressive complex 1 (PRC1)-associated protein (CBX4 protein) that is a member of the Polycomb group (PcG) of proteins[7]. PcG proteins are transcriptional repressors that are mainly involved in regulating development, senescence, stemness, and cancer progression[8]. The balance in PcG gene penetrance is crucial for proper stem cell homeostasis and the prevention of CSC development. CBX4, a SUMO E3 ligase, is different from other members of the CBX family and prevents human epidermal stem cells from entering senescence and contributes to maintenance of their stemness[7]. CBX4 increases the transcriptional activity of HIF-1a and hypoxia-induced VEGF expression and angiogenesis by promoting HIF-1a SUMOylation[9]. In addition, we previously reported that high CBX4 expression predicts poor OS in patients with HCC[10], which suggests CBX4 as an independent prognostic factor for HCC patients who received postoperative transarterial chemoembolization treatment[11]. Taken together, these results indicated that CBX4 may play a role in maintaining CSCs in HCC.

miRNAs have been identified as oncogenes or tumor suppressor genes in regulating the progression of cancers. Recently, several miRNAs have been demonstrated to be associated with sorafenib resistance and to function as predictive biomarkers for the outcome of HCC patients receiving sorafenib treatment[12–15]. For example, in HCC animal models, miR-221 upregulation is considered to be a molecular event associated with resistance to sorafenib. Thus, patients with low circulating miR-221 respond to sorafenib[13]. Meanwhile, other studies have shown that some miRNAs are associated with the regulation of cancer stem cells. For example, miR-613 inhibits liver CSC expansion by regulating the SOX9 pathway[16]. Our previous study also showed that multiple miRNAs, including let-7c, miR-200b, miR424 and miR-222, are essential to maintaining stem cell-like properties by regulating PBX3[17].

In this study, we demonstrated that miR424 could regulate CBX4 expression to maintain stem cell-like properties in sorafenib-resistant (SR) cells, and CBX4 overexpression was positively associated with the HIPPO-YAP pathway in SR cells. Increasing CBX4 levels in HCC cells enhances HIF1α-dependent YAP nuclear translocation and induces sorafenib resistance, but blocking CBX4 and YAP1 with the CBX4 inhibitor UNC3866 and the YAP1 inhibitor CA3 significantly suppresses tumor cell growth and CSC properties, particularly in SR cells. In brief, our findings indicate that CBX4 is essential for tumorigenesis by initiating YAP function in the nucleus to maintain CSC capabilities and is a good therapeutic target for preventing and treating tumors as well as evaluating the prognosis in patients with SR HCC.

2. Materials And Methods

2.1 Cell lines and plasmids

The human HCC cell lines PLC and Huh7 were cultured in RPMI 1640 (Gibco, Grand Island, NY, USA) supplemented with 10% fetal bovine serum (FBS), 100 IU/mL penicillin and 100 μg/mL streptomycin at 37 °C with 5% CO_2 in a humidified atmosphere. The identities of the cell lines were verified by DNA fingerprinting, which was performed by short tandem repeat (STR) DNA profiling. 106 paired tumor and adjacent nontumor samples were obtained from HCC patients who underwent hepatectomy with an agreement at the Department of Hepatology Surgery from the ATH of XJMU (Affiliated Tumor Hospital of Xinjiang Medical University). The acquisition and use of these tissues were permitted based on the acquisition of informed consent according to the protocol approved by the Ethics Committee (no. G-201419). Validated pCDNA3.1-CBX4 and PLKO.1-shCBX4 (5'-CCGGCGTGATCGTGATGAGCAAATACTCGAGTATTTGCTCATCACGATCACGTTTTTG-3') plasmids were kindly gifted by Professor Tiebang Kang from Sun Yat-sen University Cancer Center, Guangzhou, China, and cloned into the lentivirus shuttle vector plenti6 (Invitrogen). Various lentiviruses were packaged in 293T cells by ViraPower Packaging Mix (Invitrogen) according to the manufacturer's instructions as described in our previous study[18].

2.2 Establishment of sorafenib-resistant cell lines

To establish SR subclones, Huh7 and PLC parental cells were cultured with various concentrations of sorafenib for 6 weeks, and surviving cells were passaged 4 times and constantly incubated with 10 μmol/L sorafenib. The establishment of these resistant subclones was conducted prior to performing the experiments.

2.3 Cell growth inhibition assay

SR cells and their corresponding parental cells were cultured in 96-well plates with 0.0001–100 μmol/L sorafenib for 72 hours. Cell viability was then assessed using the CellTiter 96 aqueous nonradioactive cell proliferation assay (MTS) according to the manufacturer's instructions (Promega). The results are presented as the percentage of control and were repeated at least 3 times.

2.4 The luciferase reporter assay

The 3'-UTRs of CBX4 carrying the putative miR424 binding sites or mutant binding sites were amplified by PCR and inserted immediately downstream of the firefly luciferase cDNA in the pGL3-control vector (Promega, Madison, WI, USA) to construct pGL3-CBX4 WT and pGL3-CBX4 MUT. Briefly, 10^5 cells per well were seeded in 24-well plates, and 300 ng of pGL3 constructs plus 26 ng of pRL-TK plasmid that expressed Renilla luciferase were cotransfected with 60 pmol of miR-424 mimics or miR-424 mimics-control (GenePharma) using Lipofectamine 2000 (Invitrogen). After transfection for 48 hours, the luciferase activity was measured using a Dual-Luciferase Assay kit (Promega). The data for each sample were normalized to Renilla luciferase activity, and three independent experiments were performed.

2.5 RNA extraction and quantitative real time-polymerase chain reaction (qRT-PCR)

Total RNA was extracted from cultured cells using QIAzol (Qiagen, Hilden, Germany) for both miRNA and mRNA analyses. For mature miRNA quantification, 1 μg of total RNA was subjected to the addition of poly(A) tails by poly(A) polymerase (NEB, Beverly, MA, USA), followed by reverse transcription with an oligo (dT) adaptor primer. For mRNA detection, cDNAs were synthesized from 4 μg of total RNA using oligo (dT15) primers. For the analysis of mature and CBX4, quantitative RT-PCR (qRT-PCR) was performed using the above cDNA with SYBR Green PCR Master Mix (Applied Biosystems, Foster City, CA) and the appropriate primers (nucleotide sequences are provided in Table S1) on an ABI Prism 7500 Fast (Applied Biosystems) according to the manufacturer's instructions as previously reported. Data are presented as relative quantification (RQ) to U6 or GAPDH based on calculations of $2^{-\Delta Ct}$ where ΔCt = Ct (Target) − Ct (Reference). Fold change was calculated by the $2^{-\Delta Ct}$ method.

2.6 Spheroid formation assay

To assay sphere formation efficiency, 100 cells per well in a single-cell suspension were plated in ultra-low attachment 96-well plates (Corning Incorporated Life Science, Acton, MA, USA) and cultured in 100 μL of 1:1 mix of 2% methylcellulose (Sigma) and Dulbecco's modified Eagle's medium/F12 supplemented with 50 ng/mL epidermal growth factor (EGF), 50 ng/mL basic fibroblast growth factor (FGF), 10 ng/mL hepatocyte growth factor (HGF) and B27 (1:50) (Invitrogen) according to the protocol as previously reported[6]. After the plates were incubated at 37 °C under a 5% CO_2 atmosphere for 2–3 weeks, the spheres > 100 μm in diameter were counted under a stereomicroscope (Olympus, Tokyo, Japan)

2.7 Western blot analysis

Total protein was extracted from cultured cells using RIPA (ShineGene Molecular Biotech, Inc., Shanghai, China) according to the manufacturer's instructions. SDS–PAGE and Western blotting were performed using standard protocols. The primary antibodies and the secondary HRP-conjugated goat anti-mouse or anti-rabbit antibodies used as well as the corresponding dilutions are listed in Table S2. Signals were detected using the Immobilon™ Western Chemiluminescent HRP substrate (Millipore).

2.8 Indirect immunofluorescence staining

Huh7 and genetic cells as well as primary cancer tissues were subjected to indirect immunofluorescence staining with YAP1 (1:100), HIF1α(1:100) and CBX4 (1:100) primary antibodies followed by labeling with Alexa-488 (for CBX4 or HIF1a and YAP) and Rhodamine (for YAP1) as described elsewhere[19]. Nuclei were stained with 4,6-diamidino-2-phenylindole dihydrochloride (DAPI, Polysciences, Warrington, PA, USA) at 0.5 μg/mL. All specimens were mounted in 90% glycerol/PBS with 2.5% 1,4-diazabicyclo (2, 2, 2) octane and assayed by confocal microscopy (SP5, Leica, Wetzlar, Germany).

2.9 In vivo xenograft mouse model

To establish a tumor-bearing mouse model in order to assess tumorigenicity, a dilution series of Huh7, Huh7-SR, PLC and PLC-SR cells were mixed with an equal volume Matrigel (10 mg/ml, BD, Biosciences, Bedford, MA, USA), and 100 μL of the suspensions was s.c. injected into the backs of 4- to 6-week-old NOD/SCID mice (Vital River Laboratory Animals, Beijing, China). Approximately 10 weeks later, the frequency of tumor formation was calculated based on extreme limiting dilution analysis using the webtool at http://bioinf.wehi.edu.au/software/elda/[20]. Tumor tissues were sectioned and frozen at -80 °C. To measure tumor growth, all SR and parental cells (10^6 cells in each mouse, random 5 mice for each group) were s.c. injected into mice for 3 weeks; when the tumor volume reached > 50 mm^3, 10 mg/kg/day sorafenib was administered via p.o. injection for 9 days. To detect the effects of CBX4 and YAP inhibitors, mice bearing Huh7-SR xenografts underwent i.p. injection of CA3 at 1 mg/kg [21], UNC3866 at 10 mg/kg[22], or both drugs every 2 days for a total of 2 weeks. All tumor growth was monitored 3 times a week. Mice were sacrificed, and the tumors were dissected at the end point. All animal experiments were approved by PUCH and conformed to the regulatory standards of PUCH on Laboratory Animals Care and Use in accordance with the National Institutes of Health Guide (Guide for the Care and Use of Laboratory Animals, 2011).

2.10 Statistical analysis

All data in the figures are presented as the mean ± SD, in which data are presented as indicated. The significance of differences between two groups was determined using a two-sided Student's t-test unless otherwise specified. In case of multiple tests, one-way ANOVA followed by Bonferroni-Holm procedure was applied. Survival curves for patients were plotted using the Kaplan-Meier method, with the Mantel-Cox test for statistical significance. All data were analyzed with SPSS 20.0 statistical software (IBM, Chicago, IL, USA). $p < 0.05$ was considered statistically significant.

3. Results

3.1 Sorafenib-resistant cells highlight the CSC properties of HCC

To assess whether resistance occurs in HCC therapeutically treated with sorafenib, we established the SR cell lines Huh7-SR and PLC-SR. As shown in Fig. 1A, compared with the parental controls, Huh7-SR (from 1.54 ± 0.18 μmol/L to 50.9 ± 1.7 μmol/L) and PLC-SR (from 2.561.54 ± 0.37 μmol/L to 56.9 ± 1.8 μmol/L) had significantly enhanced proliferation in the presence of sorafenib in a dose-dependent manner. Using 3D culturing, sorafenib resistance facilitated sphere formation in both Huh7-SR and PLC-SR cells (Fig. 1B), and secondary tumor formation was also remarkably increased (Fig. 1C). Furthermore, the self-renewal tumor formation capability in vivo was performed by detecting CSC properties in cells with sorafenib resistance (Fig. 1D). The frequency of successful transplantation of the diluted series of cells was affected by sorafenib resistance (Table S3). The tumor-forming ability of Huh7-SR and PLC-SR cells was dramatically increased both in vitro and in vivo. In addition, the expression of a panel of stem cell-like genes such as *OCT4, NANOG*, and *SOX2* and the ATP-banding transfer genes *ABCG2, ABCC1*, and

ABCB1 was highly amplified in Huh7-SR and PLC-SR cells compared with their parental controls as measured by qRT-PCR (Fig. 1E-F). Furthermore, Stem-like proteins were upregulated both in Huh7-SR and PLC-SR cells by Western blot (Fig. 1G). Moreover, stem cell markers, CD44 and CD133 were performed to detect the expression on the surface of difference cells between Control and SR groups (Fig. 1H). It shows that sorafenib resistance cells have occupied more CSC cells. These data indicate that sorafenib resistance induces HCC stem cell-like characteristics and enhances HCC tumorigenesis.

3.2 CBX4 is related to sorafenib resistance

A previous study revealed that CBX4 served as a novel prognostic predictor and contributed to the strategy of HCC therapy[10]. However, we don't fully know the relationship between CBX4 and sorafenib resistance. In this study, we tested RNA sequencing between Huh7-SR and PLC-SR cells and their respective parental cells to identify epigenetic changes related to sorafenib resistance. A heat map was generated, and top genes that exhibited overall upregulation in SR cells were identified. Interestingly, CBX4 was upregulated 5.28-fold in Huh7-SR cells (6th of 442 upregulated genes, logFC > 2, P < 0.05) and 2.7-fold in PLC-SR cells (9th of 260 upregulated genes, logFC > 2, P < 0.05) (Fig. 2A). Hence, we decided to transduce CBX4 into SR and parental cells in different ways to find a correlation between CBX4 expression and sorafenib resistance. With full-length CBX4 cloned into a lentivirus system for obtaining cells with stable overexpression of CBX4, we found that CBX4 overexpression drives more proliferation in the presence of 0.001-500 μm/mol sorafenib (Fig. 2B). In contrast, knockdown of CBX4 was used to test the sorafenib-dependent influence on proliferation (Fig. 2C). This evidence implicated a correlation between CBX4 and sorafenib resistance, as described in Table S4.

3.3 miR424 mediates the suppressive effect on CBX4 gene expression

To gain insight into the reaction of CBX4-induced sorafenib resistance, miRNA sequencing analysis between SR and parental cells was performed to confirm which miRNAs were up- or downregulated in response to sorafenib resistance. In addition, 226 miRNAs and 203 miRNAs were significantly downregulated in PLC-SR and Huh7-SR, respectively. Based on miRNA website analyses (miRbase, TargetScan and http://www.microrna.org/microrna), miR424 is a candidate upstream regulator of CBX4 that affects the response to sorafenib resistance (Fig. 2D). To understand whether CBX4 is a direct target of miR424, a luciferase reporter assay was performed with vectors containing the 3'-UTR of CBX4 with the putative binding sites of miR424 (Fig. 2E, Up). Compared to co-transfection of the 3'UTR with miR-WT or miR-Mut, transfection of the 3'UTR with miR424 led to a significant decrease in luciferase activity in 293FT cells (Fig. 2E, Down). Furthermore, qRT-PCR analysis confirmed that CBX4 expression decreased by approximately 77.3% and 65.9% in miR424 overexpressed Huh7 and PLC cells, respectively, compared with corresponding control cells (Fig. 2F). This inverse relationship between miR424 and CBX4 mRNA is causal because ectopic miR424 expression reduced CBX4 mRNA levels, whereas treatment with an miR424-TUD blocked the upregulation of CBX4 mRNA (Fig. 2G). To further assess the function of miR424

in cells regarding the rescue of CBX4-induced sorafenib resistance, we measured the IC50 value of sorafenib in CBX4-overexpressing Huh7 and PLC cells and CBX4 knockdown Huh7-SR and PLC-SR cells, even after additionally infected with miR424 or miR424 TUD. As shown in Table S5, miR424 definitely increased the resistance of HCC cells to sorafenib through CBX4 interaction. These data demonstrate that ectopic expression of miR424 downregulates the endogenous expression of CBX4 and then enhances sorafenib drug sensitivity in HCC.

3.4 Clinicopathologic characteristics and bioinformatics analysis of miR424

Because we demonstrated that miR424 remarkably contributes to stem cell-like properties in HCC[17], the relative expression data of miR424 in a total of 106 cases were further analyzed. It was shown that miR424 negatively correlated with the mRNA level of CBX4 (r=-0.346, p = 0.003) (Fig. 3A). Relative to the expression of U6, the level of miR424 was significantly downregulated in HCC tissues compared with matched adjacent normal tissues (Fig. 3B). To determine the correlation between the clinicopathological characteristics and the levels of miR424 in HCC, the data of all the included patients are summarized (Table S6). No significant correlation was observed between miR424 expression levels and gender, age or venous invasion. However, miR424 expression in the HCC tissues with local tumor cirrhosis was significantly lower than that in tissues without tumor cirrhosis (Fig. 3C). Additionally, miR424 expression was markedly decreased in tumors > 5 cm (Fig. 3D). Next, we analyzed Kaplan-Meier curves and discovered that miR424 expression is associated with longer mean OS and disease-free survival (DFS) in HCC patients (Fig. 3E-F). Using data from the TCGA database and running it through the LinkedOmics website, we validated the high expression of miR424, which was negatively and significantly associated with tumor purity (Fig. 3G), as well as its correlation with good OS outcomes (Fig. 3H). These results suggest that low miR424 expression might be a candidate indicator of poor prognosis in HCC patients.

3.5 miR424 suppresses proliferation by inhibiting CBX4-induced sorafenib-resistant cells in a xenograft nude mouse model

To evaluate whether CBX4 and its upstream regulator miR424 affect sorafenib resistance in HCC in vivo, we examined tumor growth with variant genetically altered cells by constantly treating mice with sorafenib (10 mg/kg/day) via oral administration for 9 days. As shown in Fig. 4A-B, the growth of Huh7-SR cells was dramatically increased compared with that of the Huh7 parental cells. This tumor proliferation was significantly suppressed by approximately 62% and 70% upon treatment with miR424 and CBX4 shRNA, respectively, although the percentage of tumor inhibition by treatment with both miR424 and shRNA was varied (Fig. 4C). Furthermore, CBX4 overexpression in Huh7 rapidly drives tumor growth; however, this characteristic was specifically inhibited by as much as 85% when Huh7 CBX4-overexpressing cells were treated with miR424 (Fig. 4D). Immunofluorescence showed that CBX4 is weakly expressed in the nuclei of Huh7 cells in response to sorafenib treatment but is still maintained in

the nucleus of Huh7-SR cells even in the presence of sorafenib (Fig. 4E). Furthermore, HE and immunohistochemistry were performed to validate CBX4 expression in paraffin-embedded tumor tissues from mice (Fig S1 and Fig. 4F). The immunoreactivity for CBX4 in the cytoplasm and nucleus of the CBX4 overexpress group was much stronger than that in control Huh7 cells after sorafenib treatment and was highly downregulated upon CBX4-miR424 overexpression group. These results demonstrated that miR424 plays a critical role in inhibiting CBX4 expression during the progression of sorafenib resistance in HCC.

3.6 Hippo-YAP associates with CBX4 by clustering the signal pathway

To further understand the signaling pathway involved in the response to sorafenib resistance in HCC, RNA sequencing data between Huh7-CBX4 cells and control cells were analyzed by KEGG. Three conditions (percentage of whole genes, number index of signaling genes and p value of each pathway) were considered to find the signal pathway candidates that influence sorafenib resistance. Several cell signaling pathways were enriched in SR cells. Interestingly, the Hippo pathway, Toll-like receptor pathway, ERBB pathway, etc. were clustered into the top 5 (Fig. 5A). Because the Hippo pathway was the most enriched in CBX4 cells, the mRNA level of Yap1, as well as of several other signaling molecules, was detected by qRT-PCR in CBX4-overexpressing cells. Unfortunately, compared with *NF-κB, PPARD, GLI1* and *HES1*, *YAP1* was not obviously upregulated by CBX4 (Fig. 5B). Similarly, YAP1 was not sufficiently suppressed in CBX4 knockdown cells (Fig. 5C). To clarify that the Hippo-YAP pathway is a reasonable target of CBX4, the downstream genes of YAP[23], *CTGF, AREG, BIRC5, CYR61, SOX2, OCT4*, and *NANOG*, were also verified in the same manner (Fig. 5D). Extracting the proteins from cell nucleases, YAP and stem associated factors were upregulated in CBX4 overexpressed cells by Western blot analyses (Fig. 5E). In addition, YAP1 expression in the nucleus increases with sorafenib resistance; however, it can be rescued by knockdown of CBX4 (Fig. 5F). Furthermore, expression of Flag-tagged CBX4, or Flag-tagged YAP1 in HEK 293FT cells showed that the reason of CBX4 addressing YAP or HIF1α to nuclear translocation was dependent on protein-protein interaction, as determined by Immunoprecipitation and immunoblotting analyses (Fig. 5G). These data suggest CBX hereby affect the location of YAP protein but not the production.

3.7 Targeting YAP and CBX4 inhibits tumor formation

To identify the functional role of CBX4 and YAP in HCC, the CBX4 inhibitor UNC3866 and the YAP inhibitor CA3 were used to evaluate tumor sphere formation in vitro. Both inhibitors reduced self-renewal ability and sorafenib-induced tumor formation (Fig. 6A). Moreover, associated proteins, such as HIF1α, YAP1 and stem-like genes associated with CSC properties (SOX2, NONAG and BMI1), in the cell nucleus were tested by Western blot (Fig. 6B). Furthermore, tumor growth in NOD/SCID mice was assessed after i.p. injection with 10 mg/kg/day UNC3866 and 1 mg/kg/day CA3. Both treatments significantly decreased Huh7-SR tumor growth (Fig. 6C). The combination of UNC3866 and CA3 dramatically inhibited sorafenib

resistance based on tumor volume measurements collected every 2 days and the wet weight of the tumor (Fig. 6D-E). Double immunofluorescence staining for CBX4 and YAP1 expression in Huh7-SR tumors with or without treatment with their inhibitors was also conducted, and the expression of CBX4 and YAP was as prominent in the nucleus as it was in the cytoplasm in SR tumors (Fig. 6F). However, after treatment with the inhibitors, YAP expression was decreased in the nucleus, but YAP production in cytoplasm was not affected. Similarly, CA3 reduced the nuclear translocation of CBX4 but did not interfere with CBX4 protein levels. When combined, UNC3866 and CA3 could dramatically downregulate CBX-YAP signaling. Additionally, the co-localization of YAP1 and HIF1α in nucleus in Huh7-SR cells was validated by immune-fluoresces assay and the level of HIF1α was decreased by UNC3866 treatment (Figure S3). Altogether, these data confirm CBX4 and YAP as two targets of sorafenib resistance and indicated a key role in maintaining the CSC properties of HCC; this activity is illustrated in Figure S4.

4. Discussion

Drug resistance is a serious cause of therapeutic failures in HCC. In addition to surgical treatment, sorafenib and regorafenib are two critical chemotherapies for patients whose disease progresses toward advanced HCC over a 10-year period or continuously for 3 years[4, 24]. Despite the proven efficacy of sorafenib to significantly increase OS in patients[3], the constantly effective responses for patients are not long appreciated for halting disease progression because advanced HCC often develops resistance to antiproliferative therapies[25]. In the present study, we established two drug-resistant cell lines to further explore the mechanism of sorafenib resistance with the goal of elucidating candidate targets for improving the efficacy of HCC therapy.

The relationship between CSC properties and sorafenib resistance has been predicted and highlighted in recent reports. CSC traits drive tumorigenicity in HCC cells and lead to HCC recurrence and sorafenib resistance[26]. However, SR HCC is causally linked to the maintenance of stem-like properties[27]. Enriched spheres with SR signatures have been related to CSCs, metastasis, and recurrence of HCC[28]. These findings provide us with confidence in defining the correlation between SR cells and CSC traits as well as demonstrate the self-renewal and tumor formation of serially diluted transplanted SR HCC cells.

Recent studies have revealed that a series of miRNAs are involved in HCC tumor development. For example, miR367, miR223, miR494, miR221 and miR622 expression levels were increased with sorafenib resistance in HCC cells and associated with different pathways, such as the RAS-ERK pathway, PI3K-AKT pathway, mTOR pathway, etc.[13–15, 29, 30]. However, miR-122 and miR137 expression significantly inhibited SR cells by reducing apoptosis through the AKT/ERK pathway[31] and tumor-initiating cell phenotypes[32]. Although these augmented miRNAs have been characterized to have antiangiogenic, antimetastatic and anti-stem-like functions by targeting many transcription factors in HCC, we definitively identified miR424 as a tumor repressor that targets CBX4 and is associated with poor outcomes in HCC. A previous study revealed that miR424 significantly highlights the stem-cell-like properties of HCC, while the transcription factor PBX3 responds to this activity and modulates tumorigenesis[17]. However, how miR424 is relevant to sorafenib resistance is unknown; thus, in this study, we further explored whether

miR424 governs sorafenib resistance by directly targeting CBX4 and activating CBX4-induced tumor formation and self-renewal characteristics. As previously reported, sorafenib could inhibited EGFR activity, and directly affected the downstream PI3K-YAP pathway [33]. Nevertheless, the interaction between PI3K and YAP has not been sufficiently explained. Based on the correlation between PI3K and miR424[34, 35] and this study, we give one explanation of PI3K /YAP interactivity through miR424-CBX4 which was induced by sorafenib resistance. But, the mechanism of how miR424 was regulated by PI3K was needed further understand in the feature.

Because we reported that cytoplasmic CBX4 protein levels indicated poor survival for HCC patients who undergo surgical resection[10], CBX4 was followed by analysis of a TCGA dataset and GTEx bioinformatics with 11 public HCC expression datasets that covered approximately 3401 clinical samples (Fig S2 and Table S7)[36]. We clearly confirmed that a high CBX4 level contributes not only to tumorigenesis but also to a more advanced stage of HCC. As a factor of poor prognosis, CBX4 increases the transcriptional activity of HIF-1a and hypoxia-induced VEGF expression in HCC[9]. In addition, CBX4 results in BMI1 recruitment via its E3 sumo ligase activity[37] and has been shown to suspend proliferation and promote terminal differentiation[8]. This differential activity might be influenced by individual characteristics of different organs, as we found that CBX4 drives opposing behaviors in colorectal carcinoma metastasis[38]. In our present study, as a tumor progenitor, CBX4 was shown to induce stem-cell-like properties and promote YAP nuclear translocation in a HIF1a-dependent manner. This outcome is based on the discovery from the KEGG analysis of the sequencing data between CBX4-overexpressing cells and control cells. Thus, exciting results indicate several interesting pathways downstream of CBX4 signaling. For example, Wnt signaling has always enhanced CSC properties[39], Toll-like receptor signaling facilitates stem cell marker expression in HCC[40], and the PI3K-AKT pathway is a canonical signaling pathway downstream of EGFR to reduce tumor-initiating cell frequency[41]. The Hippo-YAP pathway showed the greatest upregulation in response to CBX4 in our results. Although HIF1a and YAP have been widely reported and contribute to CSCs in HCC[42, 43], we actually found that CBX4 regulates YAP signaling through YAP translocation rather than its production in SR HCC, and this mechanism implicates that the CBX4-YAP interaction is an important event for sorafenib resistance and even contributes to HCC therapy as shown in Figure S4.

The mounting evidence suggests that CSCs are particularly resistant to chemotherapy[44], and cells with sorafenib resistance maintain their CSC properties[27]. Our previous findings indicated that YAP1 plays a critical role in CSC self-renewal and tumor formation and that suppressing YAP1 could be an effective way to prevent the maintenance of CSCs[21]. In this study, we propose that targeting the CBX4-YAP1 axis could viable in treating CSCs and might be a novel strategy for SR HCC. Therefore, defining CBX4-YAP mediators of resistance to therapy is critical to better understand the relationship between CSC and sorafenib resistance.

We also investigated the effect of the combination of CBX4 and YAP inhibitors (UNC3866 and CA3) as a therapy for SR cells. Notably, the use of three targeted medicines for treating tumors is not available in the clinic. However, in our study, we provide effective candidates for patients who experience

chemotherapy failure but can still benefit from a long-term treatment, even if they develop sorafenib resistance. In our opinion, we suggest three ways to maintain an available strategy for sorafenib resistance: transducing cells with miRNA424, inhibiting CBX4 expression and arresting the Hippo-YAP pathway. We also propose a rational, biomarker-based clinical trial (using CBX4 and YAP1 overexpression to enrich the HCC patient cohort). We would also like to provide empirical therapeutic strategies for reducing sorafenib resistance by conducting in-depth molecular analyses of HCC.

5. Conclusion

Our data demonstrated that CBX4 is often overexpressed in HCC, especially in response to sorafenib resistance. Its mRNA expression is controlled by miR424, which affects the proliferation capacity and tumor stem-like properties of the cells. Increasing miR424 induces CBX4 disaggregation and reduces the interaction of CBX4 and HIF1a, subsequently decreasing YAP1 nuclear translocation to downregulate oncogenesis and inhibit malignant characteristics. If CBX4 and YAP1 are both inhibited, the best antitumor effect is achieved in vitro and in vivo, particularly in SR cells. Thus, these data provide compelling evidence that the CBX4-YAP1 axis serves as a novel anti-sorafenib resistance target and provide a strong rationale to explain the cause of CSC maintenance from SR cells. Importantly, these molecules are a promising therapeutic target for HCC and can be used to improve the outcome of patients.

Abbreviations

HCC, Hepatocellular carcinoma; CBX4, Chromobox Protein Homolog 4; SR, Sorafenib Resistance; CSC, Cancer Stem Cell; PBS, phosphate-buffered saline; qRT-PCR, quantitative reverse transcription-polymerase chain reaction

Declarations

Ethical Approval and Consent to participate

The acquisition and use of these tissues were permitted based on the acquisition of informed consent according to the protocol approved by the Ethics Committee (no. G-201419).

Consent for publication

Not applicable

Availability of supporting data

The dataset supporting the conclusions of this article is included within the article.

Competing interests

The authors declare that there are no conflicts of interest.

Funding

This study was funded by the National Natural Science Foundation of China (81872025、81460360 and 81772632), the Beijing Natural Science Foundation (7182030), the Clinical Features Research of Capital (No. Z151100004015173) and Natural Science Foundation of Xinjiang Uygur Autonomous Region (2015211C126). The grant from Scientific Research Foundation for Returned Scholars, Peking University Third Hospital (No. Y76476-05).

Authors' contributions

WZ, BW and BC supervised this study. BM, ZT and WZ conceived the experiments. JT selected samples an analyzed the clinical data. BW analyzed the data from the public database. WZ, BM, ZT, BD, GA and HH performed experiments, WZ and BM wrote the manuscript. All authors were involved in writing the paper and all approved the submitted manuscript.

Acknowledgements

The authors thank the staff at the Department of Cell Biology, Peking University Cancer Hospital and Institute, Beijing, China 100034, China, for technical support. Thank the Xinjiang Cancer Biobank of Tumor Affliated Hospital of Xinjiang Medical University (Urumuqi, China) for providing samples of hepatocellular carcinoma. Thank Mrs. Xinying Ma for her great artistic suggestion from Ma’s Scientific Illustration Studio, Beijing, China.

References

1. Bray F, Ferlay J, Soerjomataram I, Siegel RL, Torre LA, Jemal A. Global cancer statistics 2018: GLOBOCAN estimates of incidence and mortality worldwide for 36 cancers in 185 countries.CA: a cancer journal for clinicians, 2018, 68(6):394–424.
2. Kulik L, El-Serag HB. Epidemiology and Management of Hepatocellular Carcinoma.Gastroenterology, 2019, 156(2):477–491 e471.

3. Llovet JM, Ricci S, Mazzaferro V, Hilgard P, Gane E, Blanc JF, et al. Sorafenib in advanced hepatocellular carcinoma.The. New England journal of medicine. 2008;359(4):378–90.
4. Cheng AL, Kang YK, Chen Z, Tsao CJ, Qin S, Kim JS, et al. Efficacy and safety of sorafenib in patients in the Asia-Pacific region with advanced hepatocellular carcinoma: a phase III randomised, double-blind, placebo-controlled trial. The Lancet Oncology. 2009;10(1):25–34.
5. Park CY, Tseng D, Weissman IL. Cancer stem cell-directed therapies: recent data from the laboratory and clinic.Molecular therapy: the. journal of the American Society of Gene Therapy. 2009;17(2):219–30.
6. Zhao W, Wang L, Han H, Jin K, Lin N, Guo T, et al: 1B50-1, a mAb raised against recurrent tumor cells, targets liver tumor-initiating cells by binding to the calcium channel alpha2delta1 subunit.Cancer cell, 2013, 23(4):541–556.
7. Kagey MH, Melhuish TA, Wotton D. The polycomb protein Pc2 is a SUMO E3.Cell, 2003, 113(1):127–137.
8. Luis NM, Morey L, Mejetta S, Pascual G, Janich P, Kuebler B, et al: Regulation of human epidermal stem cell proliferation and senescence requires polycomb- dependent and -independent functions of Cbx4.Cell stem cell, 2011, 9(3):233–246.
9. Li J, Xu Y, Long XD, Wang W, Jiao HK, Mei Z, et al: Cbx4 governs HIF-1alpha to potentiate angiogenesis of hepatocellular carcinoma by its SUMO E3 ligase activity.Cancer cell, 2014, 25(1):118–131.
10. Wang B, Tang J, Liao D, Wang G, Zhang M, Sang Y, et al. Chromobox homolog 4 is correlated with prognosis and tumor cell growth in hepatocellular carcinoma. Ann Surg Oncol. 2013;20(Suppl 3):684–92.
11. Jiao HK, Xu Y, Li J, Wang W, Mei Z, Long XD, et al: Prognostic significance of Cbx4 expression and its beneficial effect for transarterial chemoembolization in hepatocellular carcinoma.Cell death & disease, 2015, 6:e1689.
12. Salvi A, Conde I, Abeni E, Arici B, Grossi I, Specchia C, et al: Effects of miR-193a and sorafenib on hepatocellular carcinoma cells.Molecular cancer, 2013, 12:162.
13. Fornari F, Pollutri D, Patrizi C, La Bella T, Marinelli S, Casadei Gardini A, et al. In Hepatocellular Carcinoma miR-221 Modulates Sorafenib Resistance through Inhibition of Caspase-3-Mediated Apoptosis.Clinical cancer research: an. official journal of the American Association for Cancer Research. 2017;23(14):3953–65.
14. Xu J, Lin H, Li G, Sun Y, Chen J, Shi L, et al: The miR-367-3p Increases Sorafenib Chemotherapy Efficacy to Suppress Hepatocellular Carcinoma Metastasis through Altering the Androgen Receptor Signals.EBioMedicine, 2016, 12:55–67.
15. Dietrich P, Koch A, Fritz V, Hartmann A, Bosserhoff AK, Hellerbrand C. Wild type Kirsten rat sarcoma is a novel microRNA-622-regulated therapeutic target for hepatocellular carcinoma and contributes to sorafenib resistance.Gut, 2018, 67(7):1328–1341.

16. Li B, Liu D, Yang P, Li HY, Wang D. miR-613 inhibits liver cancer stem cell expansion by regulating SOX9 pathway.Gene, 2019, 707:78–85.
17. Han H, Du Y, Zhao W, Li S, Chen D, Zhang J, et al: PBX3 is targeted by multiple miRNAs and is essential for liver tumour-initiating cells.Nature communications, 2015, 6:8271.
18. Zhang Y, Zhao W, Li S, Lv M, Yang X, Li M, et al: CXCL11 promotes self-renewal and tumorigenicity of alpha2delta1(+) liver tumor-initiating cells through CXCR3/ERK1/2 signaling.Cancer letters, 2019, 449:163–171.
19. Yang M, Liu J, Wang F, Tian Z, Ma B, Li Z, et al. Lysyl oxidase assists tumorinitiating cells to enhance angiogenesis in hepatocellular carcinoma. Int J Oncol. 2019;54(4):1398–408.
20. Hu Y, Smyth GK. ELDA: extreme limiting dilution analysis for comparing depleted and enriched populations in stem cell and other assays. J Immunol Methods. 2009;347(1–2):70–8.
21. Li F, Xu Y, Liu B, Singh PK, Zhao W, Jin J, et al. YAP1-Mediated CDK6 Activation Confers Radiation Resistance in Esophageal Cancer - Rationale for the Combination of YAP1 and CDK4/6 Inhibitors in Esophageal Cancer.Clinical cancer research: an. official journal of the American Association for Cancer Research. 2019;25(7):2264–77.
22. Stuckey JI, Dickson BM, Cheng N, Liu Y, Norris JL, Cholensky SH, et al. A cellular chemical probe targeting the chromodomains of Polycomb repressive complex 1. Nature chemical biology. 2016;12(3):180–7.
23. Moya IM, Halder G. Hippo-YAP/TAZ signalling in organ regeneration and regenerative medicine. Nature reviews Molecular cell biology. 2019;20(4):211–26.
24. Bruix J, Qin S, Merle P, Granito A, Huang YH, Bodoky G, et al: Regorafenib for patients with hepatocellular carcinoma who progressed on sorafenib treatment (RESORCE): a randomised, double-blind, placebo-controlled, phase 3 trial.Lancet, 2017, 389(10064):56–66.
25. Jindal A, Thadi A, Shailubhai K. Hepatocellular Carcinoma: Etiology and Current and Future Drugs. Journal of clinical experimental hepatology. 2019;9(2):221–32.
26. Fan Z, Duan J, Wang L, Xiao S, Li L, Yan X, et al: PTK2 promotes cancer stem cell traits in hepatocellular carcinoma by activating Wnt/beta-catenin signaling.Cancer letters, 2019, 450:132–143.
27. Lozano E, Macias RIR, Monte MJ, Asensio M, Del Carmen S, Sanchez-Vicente L, et al: Causes of hOCT1-dependent cholangiocarcinoma resistance to sorafenib and sensitization by tumor-selective gene therapy.Hepatology, 2019.
28. Fekir K, Dubois-Pot-Schneider H, Desert R, Daniel Y, Glaise D, Rauch C, et al: Retrodifferentiation of Human Tumor Hepatocytes to Stem Cells Leads to Metabolic Reprogramming and Chemoresistance.Cancer research, 2019, 79(8):1869–1883.
29. Tang X, Yang W, Shu Z, Shen X, Zhang W, Cen C, et al: MicroRNA223 promotes hepatocellular carcinoma cell resistance to sorafenib by targeting FBW7.Oncology reports, 2019, 41(2):1231–1237.
30. Liu K, Liu S, Zhang W, Jia B, Tan L, Jin Z, et al: miR-494 promotes cell proliferation, migration and invasion, and increased sorafenib resistance in hepatocellular carcinoma by targeting

PTEN.Oncology reports, 2015, 34(2):1003–1010.

31. Xu Y, Huang J, Ma L, Shan J, Shen J, Yang Z, et al: MicroRNA-122 confers sorafenib resistance to hepatocellular carcinoma cells by targeting IGF-1R to regulate RAS/RAF/ERK signaling pathways.Cancer letters, 2016, 371(2):171–181.
32. Lu AQ, Lv B, Qiu F, Wang XY, Cao XH. Upregulation of miR-137 reverses sorafenib resistance and cancer-initiating cell phenotypes by degrading ANT2 in hepatocellular carcinoma.Oncology reports, 2017, 37(4):2071–2078.
33. Xia H, Dai X, Yu H, Zhou S, Fan Z, Wei G, et al: EGFR-PI3K-PDK1 pathway regulates YAP signaling in hepatocellular carcinoma: the mechanism and its implications in targeted therapy.Cell death & disease, 2018, 9(3):269.
34. Zhang H, Wang X, Chen Z, Wang W. MicroRNA-424 suppresses estradiol-induced cell proliferation via targeting GPER in endometrial cancer cells.Cell Mol Biol (Noisy-le-grand), 2015, 61(7):96–101.
35. Shi XH, Li X, Zhang H, He RZ, Zhao Y, Zhou M, et al. A Five-microRNA Signature for Survival Prognosis in Pancreatic Adenocarcinoma based on. TCGA DataSci Rep. 2018;8(1):7638.
36. Lian Q, Wang S, Zhang G, Wang D, Luo G, Tang J, et al: HCCDB: A Database of Hepatocellular Carcinoma Expression Atlas.Genomics, proteomics & bioinformatics, 2018, 16(4):269–275.
37. Ismail IH, Gagne JP, Caron MC, McDonald D, Xu Z, Masson JY, et al: CBX4-mediated SUMO modification regulates BMI1 recruitment at sites of DNA damage.Nucleic acids research, 2012, 40(12):5497–5510.
38. Wang X, Li L, Wu Y, Zhang R, Zhang M, Liao D, et al: CBX4 Suppresses Metastasis via Recruitment of HDAC3 to the Runx2 Promoter in Colorectal Carcinoma.Cancer research, 2016, 76(24):7277–7289.
39. Pez F, Lopez A, Kim M, Wands JR, Caron de Fromentel C, Merle P. Wnt signaling and hepatocarcinogenesis: molecular targets for the development of innovative anticancer drugs. Journal of hepatology. 2013;59(5):1107–17.
40. Liu WT, Jing YY, Yu GF, Han ZP, Yu DD, Fan QM, et al: Toll like receptor 4 facilitates invasion and migration as a cancer stem cell marker in hepatocellular carcinoma.Cancer letters, 2015, 358(2):136–143.
41. Fu W, Lei C, Yu Y, Liu S, Li T, Lin F, et al. EGFR/Notch Antagonists Enhance the Response to Inhibitors of the PI3K-Akt Pathway by Decreasing Tumor-Initiating Cell Frequency. Clinical cancer research: an official journal of the American Association for Cancer Research. 2019;25(9):2835–47.
42. Hayashi H, Higashi T, Yokoyama N, Kaida T, Sakamoto K, Fukushima Y, et al: An Imbalance in TAZ and YAP Expression in Hepatocellular Carcinoma Confers Cancer Stem Cell-like Behaviors Contributing to Disease Progression.Cancer research, 2015, 75(22):4985–4997.
43. Lai FB, Liu WT, Jing YY, Yu GF, Han ZP, Yang X, et al: Lipopolysaccharide supports maintaining the stemness of CD133(+) hepatoma cells through activation of the NF-kappaB/HIF-1alpha pathway.Cancer letters, 2016, 378(2):131–141.
44. Xiang D, Cheng Z, Liu H, Wang X, Han T, Sun W, et al: Shp2 promotes liver cancer stem cell expansion by augmenting beta-catenin signaling and predicts chemotherapeutic response of

patients.Hepatology, 2017, 65(5):1566–1580.

Figures

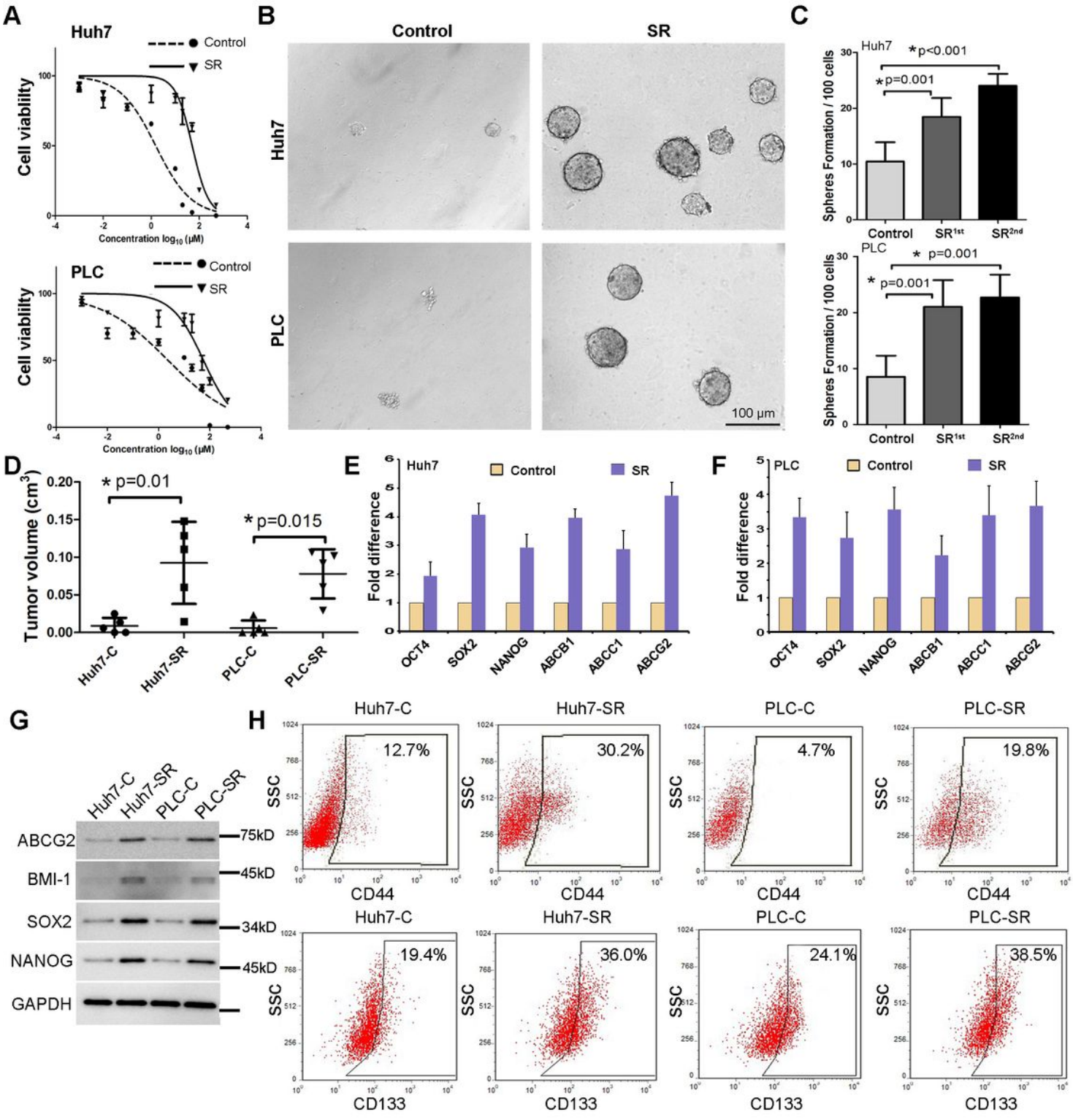

Figure 1

Sorafenib resistance induces cancer stem cell properties Huh7-SR and PLC-SR cells were established after 6 weeks of constant treatment with 10 μm/L sorafenib. MTS was performed to calculate cell proliferation based on sorafenib treatment (A). Representative phases show the spheroids formed from SR cells and parent cells (B). The ability of the spheres formed by SR cells to form secondary spheroids was also shown. Spheroids (□>100□m) were counted under a stereomicroscope (C). Serial transplantation was performed to analyze tumor growth of xenografted tumors derived from SR cells and parent cells, and the results are shown in Table S3 (D). qRT-PCR analysis of the expression of stem cell markers and drug resistance-related genes in SR and parental cells. Data are presented as the fold difference over parent cells for each gene, which was defined as E for Huh7 and F for PLC. Stem associated factors were tested by Western blot (G). CD44 and CD133 were validated between the parent and SR cells using FACS (H).

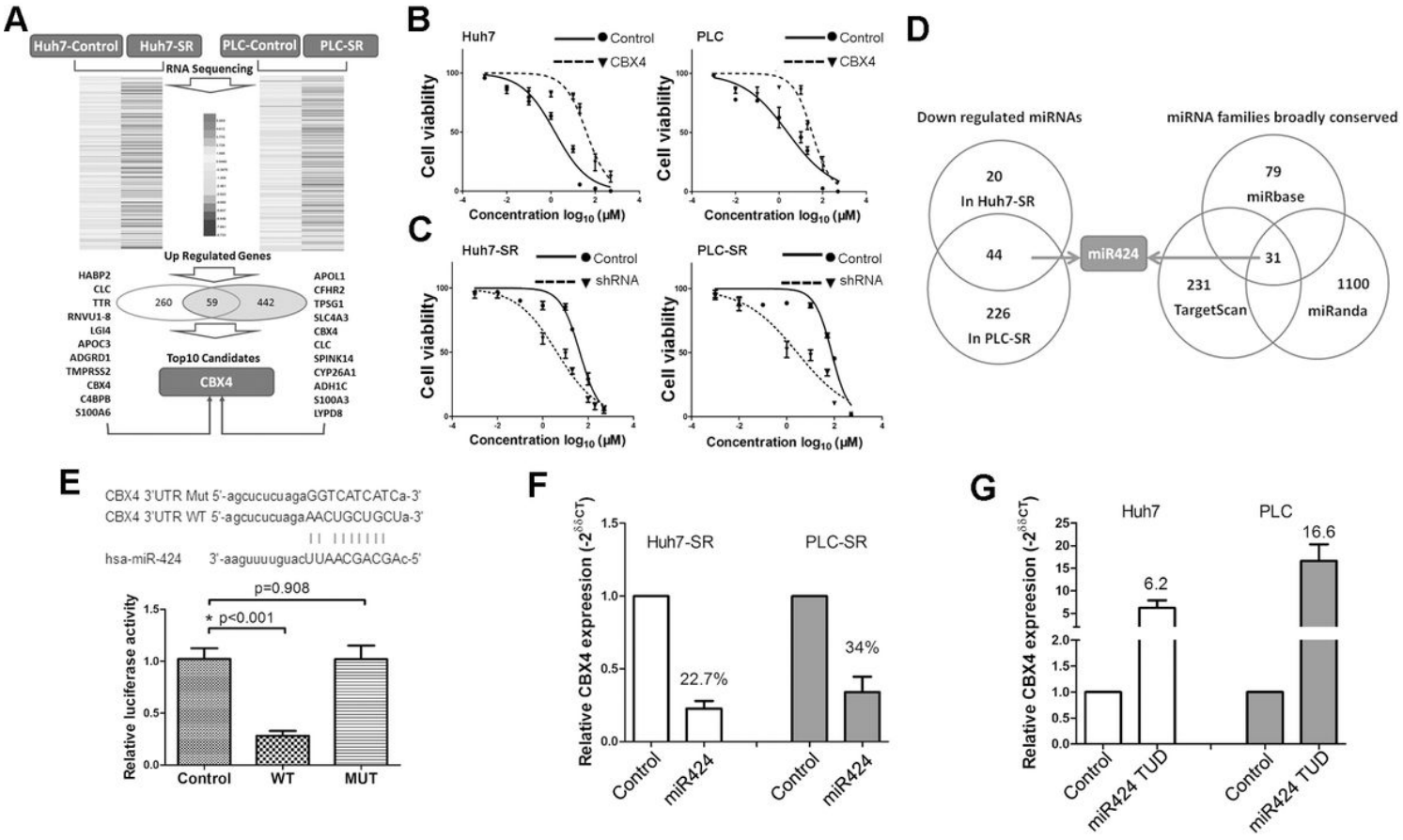

Figure 2

CBX4 and miR424 is candidates that contributes to sorafenib resistance Representative chart showing CBX4 expression based on RNA sequencing of SR cells and parent cells. CBX4 is presented as one of the top 10 selected genes from 59 total upregulated genes in both Huh7 and PLC-SR cells (A). The cell proliferation assay was performed by MTS in CBX4-modified cells and their control cells (B). Conversely, SR cells with CBX4 knockdown were more sensitive to different doses of sorafenib (C). The IC50 values are shown in Table S4. The diagram illustrates how miR424 was identified from the miRNA sequencing data and predicted by Venn screening from miRNA database websites (D). Sequence alignment of the

human miR424 seed sequence with the 3’-UTR of CBX4. The mutated sequence in the matched binding sites for the gene that was used to create the firefly luciferase reporter constructs is shown at the bottom of the gene set. A luciferase reporter assay demonstrated that miR424 inhibited the transcription of the wild-type but not the mutant 3’-UTRs of CBX4 (E). The expression of endogenous CBX4 was inhibited in miR424 overexpressed Huh7-SR and PLC-SR cells (F). In contrast, CBX4 levels were increased in Huh7 and PLC cells with miR424-TUD (G). All data were compared with the respective controls, and the mRNA level was detected by qRT-PCR. CBX4 mRNA expression was normalized to that of GAPDH mRNA; and 3 independent experiments were conducted.

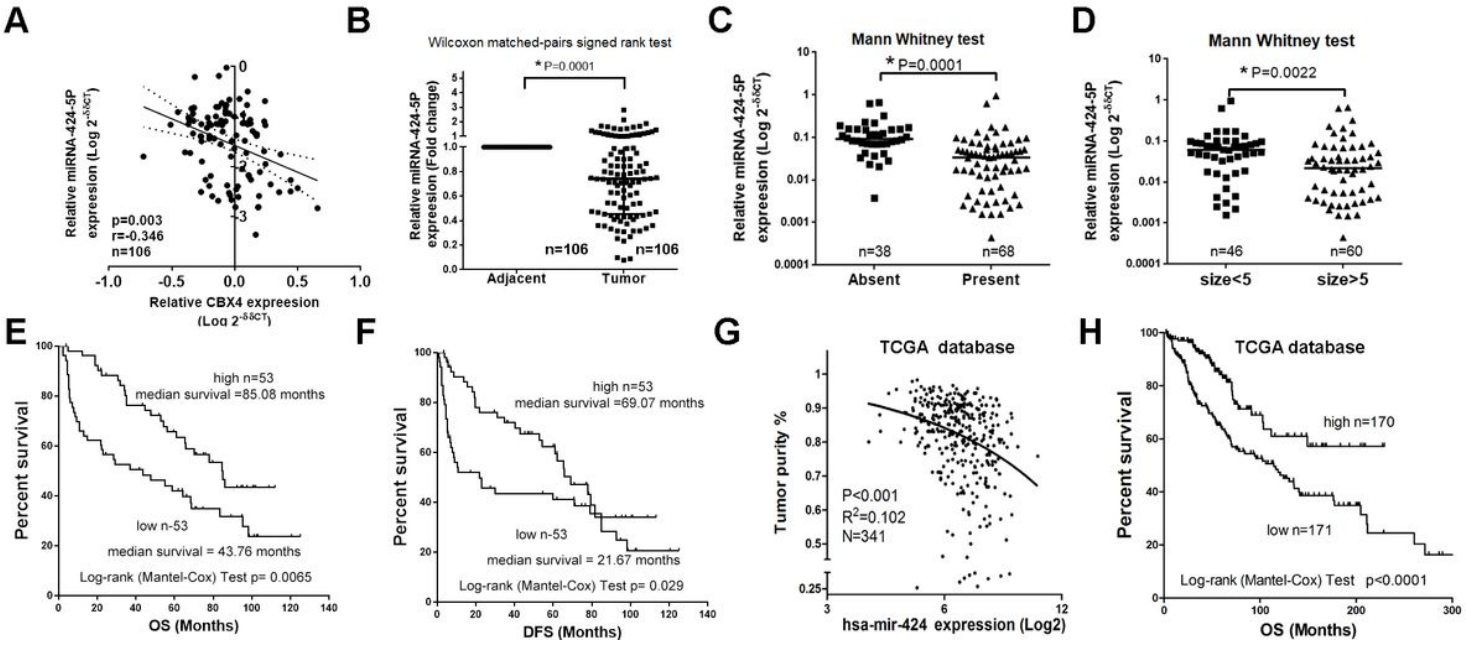

Figure 3

. miR424 expression inversely correlates with CBX4 mRNA levels in HCC tissues The negative linear regression and correlation analysis for the relation of the mRNA levels of CBX4 and those of miR424 in 106 HCC patients by qRT-PCR (A). Relative miR424 expression in HCC tissues and matched adjacent normal tissues as assessed by qRT-PCR (B). Relative expression data of miR424 in HCC cases were further analyzed. The negative relationship between miR424 expression and liver cirrhosis (C) and size (D). Kaplan-Meier curves of disease-free survival (DFS) (E) and overall survival (OS) (F). Survival of the high and low miR424 expression groups assessed using the log-rank (Mantel-Cox) test in HCC, which were divided according to a cutoff of 2.5, the median value of CBX4 mRNA expression relative to GAPDH mRNA. From the TCGA database, tumor purity was highly negatively correlated with miR424 expression (G). Linear regression and correlation between miR424 and CBX4 mRNA levels in 341 HCC tissues from the TCGA database (H).

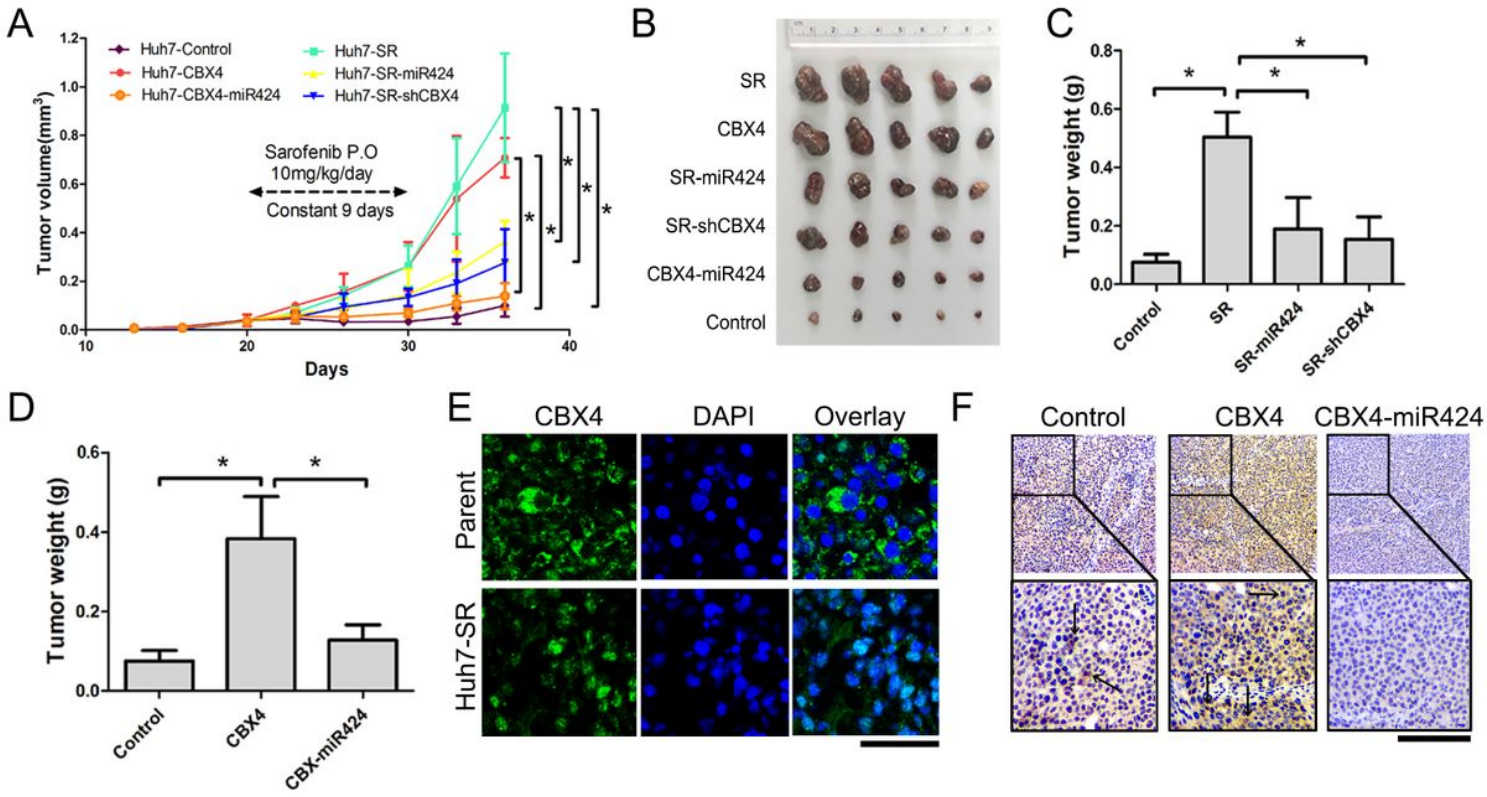

Figure 4

miR424-CBX4 affects tumor growth in a sorafenib-resistant cell-derived xenograft nude mouse model Growth curves of subcutaneous xenografts derived from various genetically altered Huh7 cells (n=5 per group) (A). Image of 5 xenograft tumors per group of Huh7 control and genetically infected cells after sorafenib treatment (B). Tumor weight was measured and showed that cells with sorafenib resistance had faster growth than did the control group (Huh7 parent cells); however, genetic inhibition of CBX4 and knockdown of miR424 prevented Huh7-SR tumor growth (C). miR424 inhibits CBX4-induced Huh7 growth (D). Representative images of immunofluorescence (IF) staining of CBX4 in frozen tumor tissues treated with sorafenib showed the different localizations of CBX4 in Huh7-SR tumors and parental cell tumors (E), bar=100 μm. Expression of CBX4 in nucleus (black arrow) and cytoplasm from paraffin-embedded tumor tissues was shown and was rescued by miR424 expression based on immunohistochemistry (F), bar=200 μm.

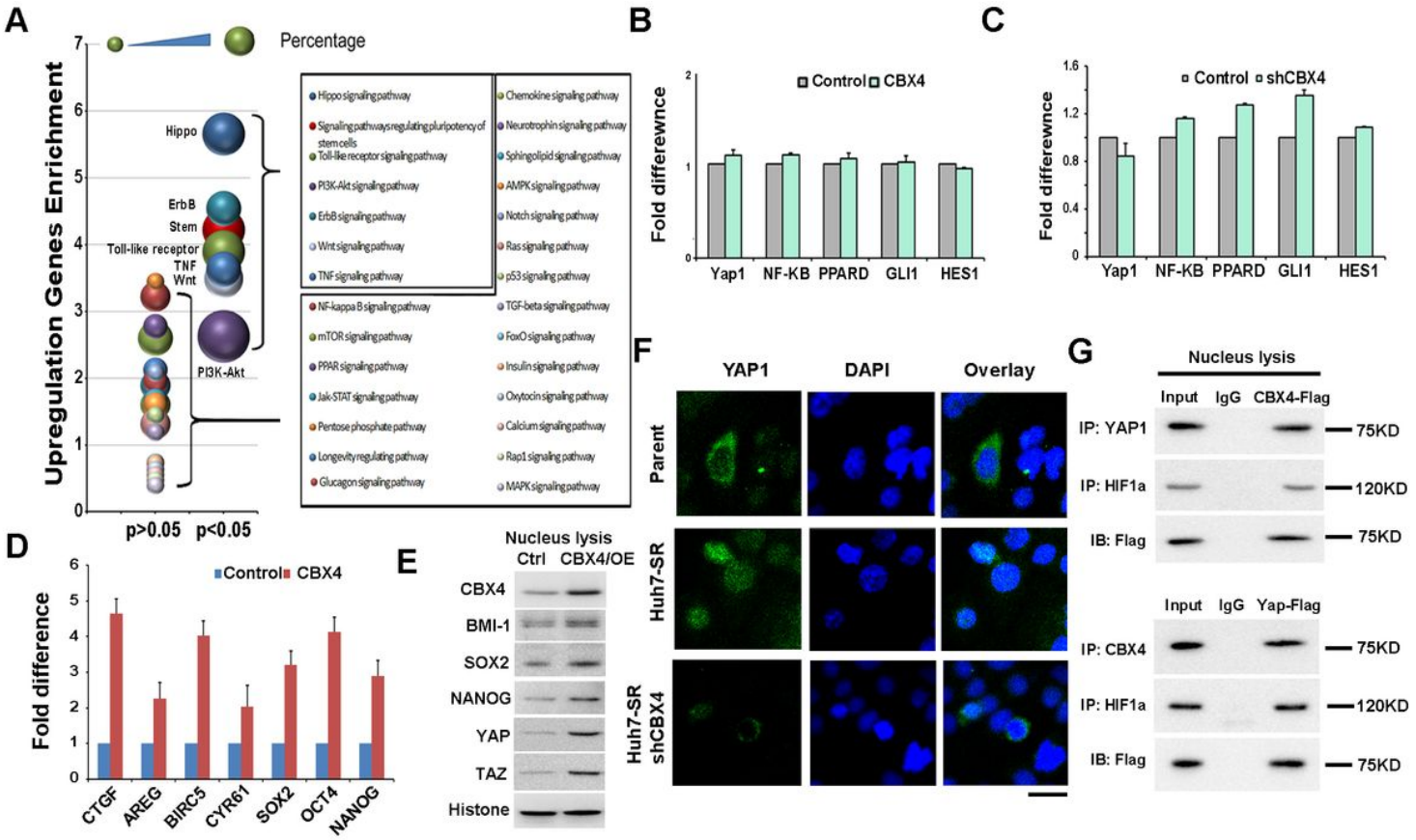

Figure 5

The Hippo-YAP pathway is an important pathway downstream of CBX4 The KEGG analysis chart shows the enriched pathways in response to unregulated genes in Huh7-CBX4 cells. The significant group of pathways is separated from a total of 28 signaling pathways; this group includes the Hippo, Toll-like receptor, ERBB, WNT, TNF, Stem-like and PI3K-AKT pathways (A). Histogram shows gene amplification by qRT-PCR in CBX4 genomic cells (B) and CBX4 knockdown cells (C). The genes downstream of the YAP pathway were amplified by qRT-PCR (D). Stem associated proteins were tested in nucleus by Western blot (E). Representative images show YAP1 expression and localization in parent cells, SR cells and SR-shCBX4 cells by IF (F), bar=100 μm. Immunoprecipitation and Immunoblotting analyses were performed with the indicated CBX4-YAP-HIF1α interaction in nucleus (G).

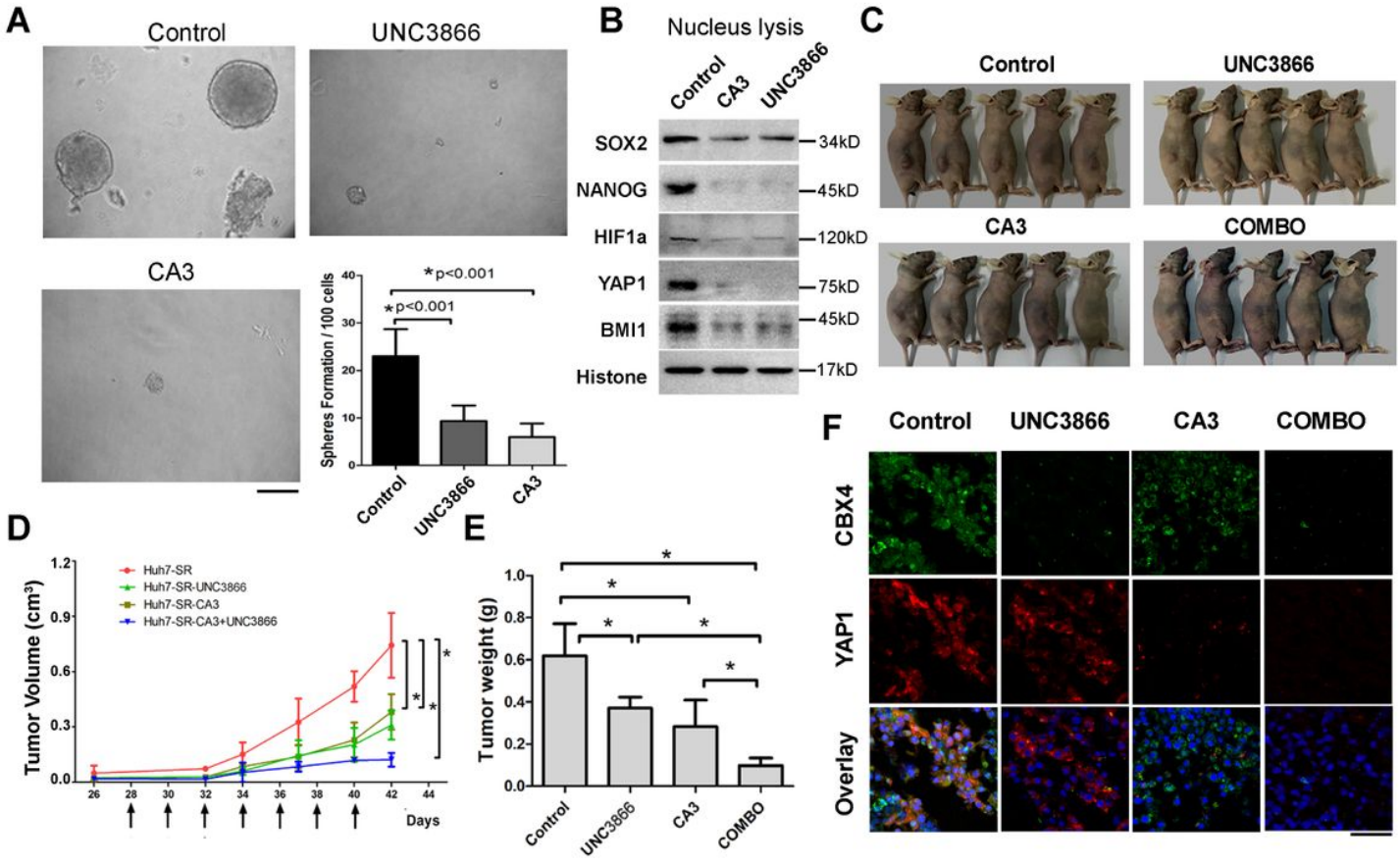

Figure 6

The combination of CA3 and UNC3866 suppresses tumorigenicity in vitro and in vivo Representative phases show the spheroids formed after treatment with CA3 and UNC3866. The ability of the cells to form spheres formed was also shown. Spheroids (Φ>100μm) were counted under a stereomicroscope, bar=100 μm (A). The protein level in the cell nucleus was validated using Western blot analysis, and histone H3 was used as an internal control (B). After tumors were visible, mice with subcutaneously transplanted Huh7-SR cells were i.p. injected with PBS+DMSO, CA3, UNC3866 or CA3 plus UNC3866 (COMBO) at the indicated doses every other day for a total of 2 weeks (C). Growth curves of Huh7-SR engraftment of each treatment group, per mouse as indicated by arrows in (D). The histogram shows the weight of the dissected tumor at experiment termination (E). * p<0.05 by Student's t-test. CBX4 and YAP1 expression and localization in frozen tumors from mice were identified by double IF (F), bar=100 μm. YAP is red; CBX4 is green; and the nucleus is blue (DAPI staining).

Supplementary Files

This is a list of supplementary files associated with this preprint. Click to download.

- FIGS2.jpg
- FIGS4.jpg

- TableS17.docx
- Supplementalfigureandtablelegend.docx
- FIGS1.jpg
- FIGS3.jpg